Macromolecules

ARTICLE

pubs.acs.org/Macromolecules

# Micellar Nanoparticles of Coil−Rod−Coil Triblock Copolymers for Highly Sensitive and Ratiometric Fluorescent Detection of Fluoride Ions

Jinming Hu,[†] Guoying Zhang,[†] Yanhou Geng,*[,‡] and Shiyong Liu*[,†]

[†]CAS Key Laboratory of Soft Matter Chemistry, Department of Polymer Science and Engineering, Hefei National Laboratory for Physical Sciences at the Microscale, University of Science and Technology of China, Hefei, Anhui 230026, China

[‡]State Key Laboratory of Polymer Physics and Chemistry, Changchun Institute of Applied Chemistry, Chinese Academy of Sciences, 5625 Renmin Street, Changchun 130022, China

Supporting Information

**ABSTRACT:** We report on the fabrication of a novel type of ratiometric fluorescent polymeric probes for fluoride ions ($F^-$) based on self-assembled micellar nanoparticles of P(MMA-*co*-NBDAE)-*b*-PF-*b*-P(MMA-*co*-NBDAE) coil−rod−coil triblock copolymer, where MMA, NBDAE, and PF are methyl methacrylate, 4-(2-acryloyloxyethylamino)-7-nitro-2,1,3-benzoxadiazole, and polyfluorene, respectively. Blue-emitting conjugated PF block and green-emitting NBDAE moieties with $F^-$ turn-off characteristics within the PMMA block serve as fluorescence resonance energy transfer (FRET) donors and switchable acceptors, respectively. For coil−rod−coil triblock copolymer in a good solvent such as THF, the blue emission of PF block dominates due to unimolecularly dissolved state associated with ineffective FRET process. The addition of $F^-$ ions only leads to ∼2.92-fold decrease of fluorescence intensity ratio, $I_{515}/I_{417}$, of characteristic NBDAE and PF emission bands. In acetone, the triblock copolymer spontaneously self-assembles into micelles possessing PF cores and NBDAE-labeled PMMA coronas. In the absence of $F^-$ ions, effective FRET processes between micellar cores and coronas occurs, resulting in prominently enhanced NBDAE emission. Upon addition of $F^-$ ions, the quenching of NBDAE emission bands leads to ∼8.75-fold decrease in the emission intensity ratio, $I_{515}/I_{417}$, which is also accompanied by naked eye-discernible fluorometric transition from cyan to blue emissions and colorimetric transition from green to yellowish. At a micellar concentration of 0.1 g/L in acetone at 25 °C, the detection limit of $F^-$ ions can be down to ∼4.78 $\mu$M (∼0.09 ppm). This work presents a new example of polymeric micelles-based optical $F^-$ probes and manifests that, upon proper structural design and optimization of spatial distribution of FRET donors and acceptors, self-assembled micelles of coil−rod−coil triblock copolymers serve as better ratiometric fluorescent $F^-$ ion sensors possessing visual detection capability, as compared to that of molecularly dissolved chains.

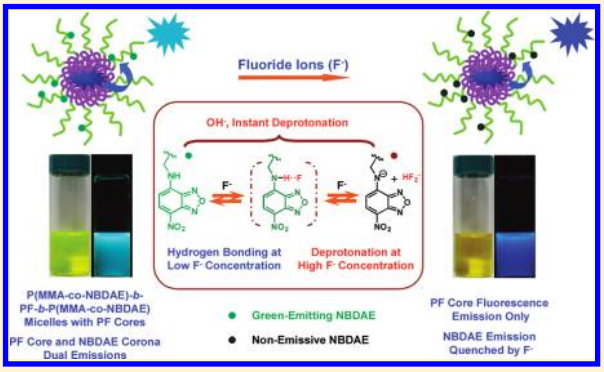


## INTRODUCTION

Anions play crucial roles in various biological, environmental, and industrial processes. Accordingly, increasing attention has been paid to the design of novel sensing and imaging systems for anions in the past decade.[1−7] In particular, fluoride ions ($F^-$) are highly relevant to health care, drinking water quality control, detection of chemical warfare agents, and refinement of uranium resources.[4,8] Up to now, three main types of strategies based on supramolecular recognition,[9−23] Lewis acid−base interactions,[24−31] and $F^-$ ion-induced chemical reaction mechanisms have been explored for the construction of colorimetric and/or fluorometric $F^-$ probes.[32−39]

Concerning supramolecular recognition-based $F^-$ chemosensors, hydrogen-bonding (HB) interactions between $F^-$ and amides, pyrroles, indoles, ureas, thioureas, ammonium, guanidinium, and imidazolium have been utilized to develop a variety of small molecule-based colorimetric and fluorometric $F^-$ probes.[9−21] We recently reported that secondary amine moieties in nitrobenzofurazan derivatives such as 4-(2-acryloyloxyethylamino)-7-nitro-2,1,3-benzoxadiazole (NBDAE) and NBDAE-containing polymers can serve as a novel type of sensitive colorimetric and fluorometric $F^-$ probes with a detection limit down to ∼0.8 $\mu$M.[40] NBDAE moieties are capable of selectively recognizing $F^-$ ions via HB interactions at low $F^-$ concentration and subjected to further deprotonation event via Brønsted acid−base interactions at high $F^-$ concentration. However, in this case, the fluorometric $F^-$ detection was based on the monitoring of intensity of a single NBDAE emission band, which is subjected to inherent limitations such as high background interference, poor repeatability, and decreased reliability due to fluctuations in detection conditions.

**Received:** August 2, 2011
**Revised:** September 9, 2011
**Published:** September 19, 2011

**Scheme 1. Schematic Illustration of P(MMA-*co*-NBDAE)-*b*-PF-*b*-P(MMA-*co*-NBDAE) Triblock Copolymer Micelles Consisting of Blue-Emitting Polyfluorene (PF) Cores and Green-Emitting P(MMA-*co*-NBDAE) Coronas, Which Can Serve as Ratiometric Fluorescent Probes for Fluoride Ions[a]**

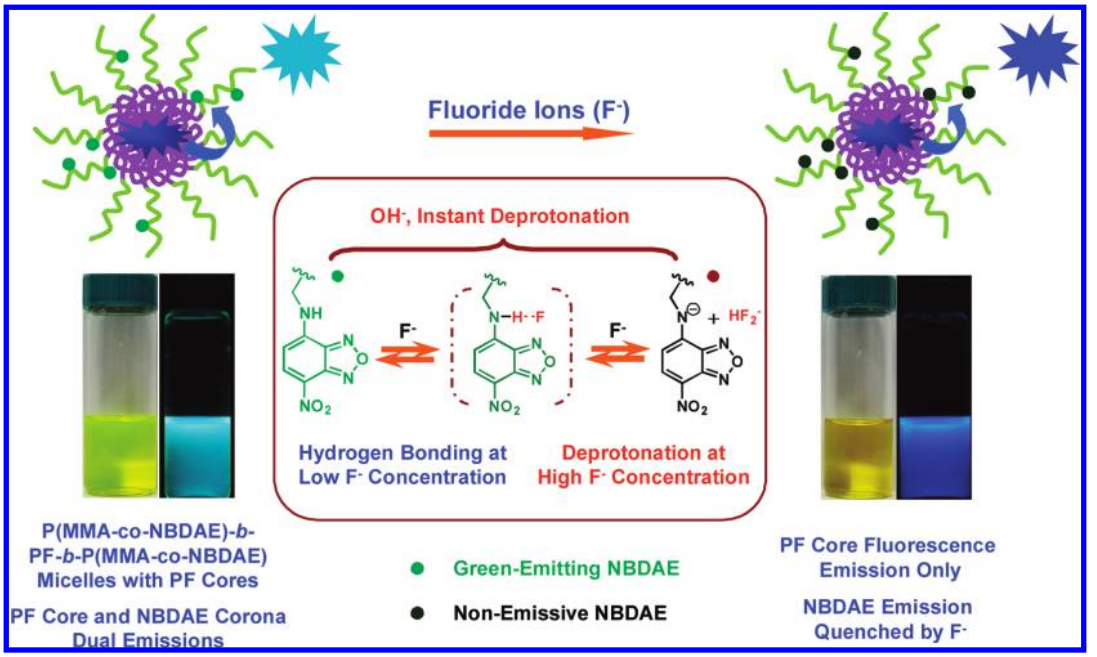


[a] In the absence of $F^-$, the FRET process between micellar cores and coronas occurs, resulting in mixed cyan fluorescence emission; in the presence of $F^-$ ions, the emission of NBDAE moieties within micellar coronas was quenched, leading to the emission of PF cores only.

Thus, the integration of an internal calibration dye is highly desirable to allow for the construction of ratiometric fluorescent $F^-$ sensing systems, leading to improved detection performances in terms of reliability, accuracy, and sensitivity.

On the other hand, compared to small molecule ones, polymeric $F^-$ sensors might offer additional advantages such as improved detection selectivity and sensitivity, structural stability, processability, and facile integration into detection devices.[41,42] In this context, Tian et al.[31,43] reported the construction of homopolymer-based fluorescent $F^-$ probes consisting of 4-benzoylamido-*N*-butyl-1,8-naphthalimide moieties. They found that the polymer molecular weight (MW) can exhibit considerable effects on the detection sensitivity. This novel type of polymeric probe also allows for $F^-$ detection in the film state. Ratiometric fluorescent $F^-$ probes can also be fabricated by employing the fluorescence resonance energy transfer (FRET) principle if a pair of donor and acceptor dyes was physically or covalently introduced into the detection system. Swager et al.[34] fabricated conjugated polymer-based ratiometric $F^-$ sensors by taking advantage of $F^-$ ion-triggered Si−O bond cleavage in side groups and the spontaneous generation of highly fluorescent coumarin moieties. In this case, amplified $F^-$ detection can be achieved via the "molecular wire" effect ascribing to the conjugated backbone.[44−46]

Recently, we have been interested in novel detection and sensing systems-based responsive polymers and their assemblies.[41,42,47] The integration of responsive polymers with small molecule sensing motifs can allow for the construction of novel type of polymeric probes possessing multifunctional sensing capability, tunable detection sensitivity and selectivity, and enhanced biocompatibility. Specifically, the introduction of FRET dye pair possessing analyte-switchable emission characteristics into responsive polymeric assemblies renders possible the external stimuli tunable spatial distribution of embedded dyes, further broadening the design flexibility, adaptability, and specific application circumstances.[41,47−57] Recently, Yang et al.[58] reported a ratiometric fluorescent $F^-$ probe from cetyltrimethylammonium bromide (CTAB) micelles-embedded small molecules via the excited-state intramolecular proton transfer (ESIPT) mechanism.

For block copolymer micelles, appropriate $F^-$ ion-inert FRET donor dyes and acceptor dyes possessing $F^-$-switchable emission characteristics, such as NBDAE, can be covalently embedded into micelle cores and coronas, respectively, allowing for the construction of ratiometric fluorescent $F^-$ probes. In addition, fluorescent conjugated polymers are well-known to be capable of coordinating the photophysical processes of a large number of side chain-attached chromophore units via efficient intrachain energy transfer mechanism and exhibiting collective properties that are sensitive to subtle external perturbation. Upon appropriate stimulation, the excitation energy along the whole conjugated polymer backbone can effectively transfer to the chromophore reporters, resulting in the amplification of fluorescence signal changes.[44−46] Thus, if fluorescent conjugated polymer segment is chosen as the core-forming block, within block copolymer micelles the close proximity of conjugated core to FRET acceptor dyes at the micellar corona can similarly take advantage of the "molecular wire" effect of conjugated polymers and allow for the construction of polymeric micelles-based effective FRET systems for sensing and imaging applications.

On the basis of our previous work of emission intensity-based fluorometric $F^-$ probes constructed from NBDAE and its polymers,[40] herein, we synthesized coil−rod−coil ABA triblock copolymers consisting of middle polyfluorene (PF) rod block and coil block of NBDAE-labeled poly(methyl methacrylate) (PMMA). In a selective solvent, the synthesized P(MMA-*co*-

**Scheme 2. Synthetic Routes for P(MMA-*co*-NBDAE)-*b*-PF-*b*-P(MMA-*co*-NBDAE) ABA Triblock Copolymer via the ATRP Technique**

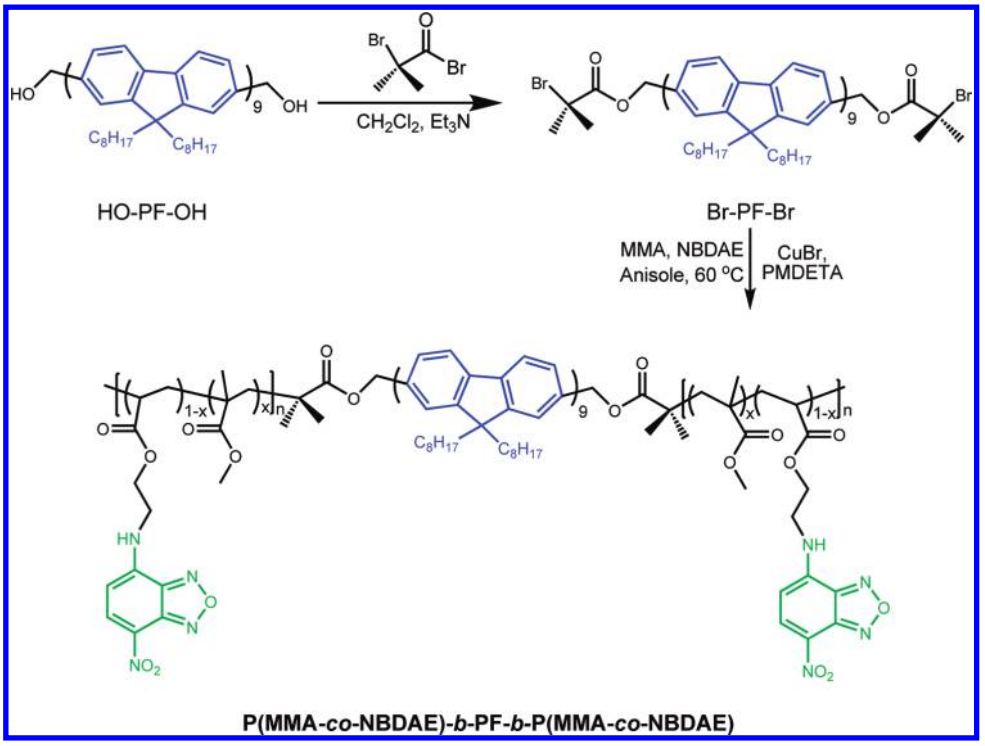


NBDAE)-*b*-PF-*b*-P(MMA-*co*-NBDAE) triblock copolymer can self-assemble into micellar nanoparticles consisting of blue-emitting PF cores and green-emitting P(MMA-*co*-NBDAE) coronas. Micelle formation will bring this pair of FRET donor and acceptor dyes into closer proximity within the formed polymeric assemblies, as compared to that for molecular dissolved triblock unimer chains (Schemes 1 and 2). We then investigated and compared the ratiometric fluorometric $F^-$ sensing capabilities of P(MMA-*co*-NBDAE)-*b*-PF-*b*-P(MMA-*co*-NBDAE) triblock copolymer in the form of self-assembled micelles and unimers. It was concluded that compared to triblock unimer chains, assembled polymeric micelles consisting of conjugated polymer cores and coronas labeled with $F^-$ ion-switchable NBDAE moieties can serve as highly sensitive and selective ratiometric $F^-$ probes with considerably enhanced sensing performances and visual detection capability.

## EXPERIMENTAL SECTION

**Materials.** Methyl methacrylate (MMA, Sinopharm Chemical Reagent Co.) was distilled over $CaH_2$ under reduced pressure. *N*,*N*,*N*′,*N*″,*N*″-Pentamethyldiethylenetriamine (PMDETA, 99%, Aldrich), 2-bromoisobutyryl bromide (98%, Aldrich), copper(I) bromide (CuBr, 98%, Aldrich), and 4-chloro-7-nitrobenzofurazan (NBD-Cl, 99%, Alfa) were used as received. 2-Aminoethanol, acryloyl chloride, and triethylamine (TEA) (Sinopharm Chemical Reagent Co.) were distilled over $CaH_2$ just prior to use. Dichloromethane ($CH_2Cl_2$) was dried over $CaH_2$ and distilled just prior to use. Tetrahydrofuran (THF), acetone, methanol, anisole, and all the other reagents were used as received. Tetra-*n*-butylammonium (TBA) salts of $Cl^-$, $Br^-$, $I^-$, $CH_3COO^-$, $ClO_4^-$, $HSO_4^-$, $H_2PO_4^-$, and $F^-$ were used as received. Dihydroxyl-terminated conjugated polyfluorene with a well-defined degree of polymerization (DP), *HO*-$PF_9$-*OH*,[59,60] and 4-(2-acryloyloxyethylamino)-7-nitro-2,1,3-benzoxadiazole (NBDAE)[61,62] were synthesized according to literatures procedures.

**Sample Synthesis.** General routes employed for the preparation of conjugated PF-based difunctional ATRP initiator, *Br*-$PF_9$-*Br*, and coil−rod−coil ABA triblock copolymer, P(MMA-*co*-NBDAE)-*b*-PF-*b*-P(MMA-*co*-NBDAE), are shown in Scheme 2.

*Synthesis of PF-Based Difunctional ATRP Initiator (Scheme 2).* Typical procedures for the synthesis of PF-based difunctional ATRP initiator, *Br*-$PF_9$-*Br*, are as follows. *HO*-$PF_9$-*OH* (0.178 g, 0.05 mmol) and TEA (14.2 mg, 0.14 mmol) were dissolved in 20 mL of anhydrous $CH_2Cl_2$ and cooled to 0 °C in an ice−water bath. 2-Bromoisobutyryl bromide (32.2 mg, 0.14 mmol) in 2 mL of dry $CH_2Cl_2$ was then added dropwise over ∼10 min. The mixture was stirred at 0 °C for 1 h and then at room temperature for another 12 h. After filtration, the filtrate was washed with saturated aqueous $NaHCO_3$ and brine solution, respectively. The organic phase was combined and then dried with anhydrous $MgSO_4$. After filtration, the solvents were removed on a rotary evaporator, affording the product as a pale yellow powder (0.16 g, yield: 83%). $^1$H NMR ($CDCl_3$, $\delta$, ppm, TMS, Figure S1): 8.02−7.34 (54H, aryl protons of PF), 5.33 (4H, PF−$CH_2$−O), 2.39−0.60 (306H, alkyl protons of PF).

*Synthesis of P(MMA-co-NBDAE)-b-PF-b-P(MMA-co-NBDAE) Triblock Copolymer (Scheme 2).* P(MMA-*co*-NBDAE)-*b*-PF-*b*-P(MMA-*co*-NBDAE) triblock copolymer was synthesized by the ATRP of MMA and NBDAE comonomers utilizing *Br*-$PF_9$-*Br* as macroinitiator and CuBr/PMDETA as the catalysts, respectively. Typically, *Br*-$PF_9$-*Br* (57.9 mg, 0.015 mmol), MMA (0.3 g, 3 mmol), NBDAE (4.2 mg, 0.015 mmol), PMDETA (5.2 mg, 0.03 mmol), and anisole (1 mL) were added into a reaction tube. The mixture was carefully degassed by three freeze−thaw cycles; CuBr (4.3 mg, 0.03 mmol) was then added under the protection of $N_2$ flow, and the tube was then sealed under vacuum. After stirring at 60 °C for 3 h, the reaction tube was opened, exposed to air, and then diluted with 5 mL of THF. After passing through a neutral alumina column and removing all the solvents on a rotary evaporator,

the residues were dissolved in THF and precipitated into an excess of methanol. The final product was dried in a vacuum oven overnight at room temperature. P(MMA-*co*-NBDAE)-*b*-PF-*b*-P(MMA-*co*-NBDAE) triblock copolymer was obtained as a yellowish powder (0.21 g, yield: 51%; $M_{n,GPC}$ = 15.3 kDa, $M_w/M_n$ = 1.13, Figure S2). The DP of P(MMA-*co*-NBDAE) block was determined to be 56 from $^1$H NMR analysis (Figure S3). Thus, the coil−rod−coil ABA triblock copolymer was denoted as P(MMA-*co*-NBDAE)$_{56}$-*b*-PF$_9$-*b*-P(MMA-*co*-NBDAE)$_{56}$. The mole content of NBDAE moieties (relative to the PMMA block) was determined to be ∼0.5 mol % based on standard UV absorption calibration curve.

*Preparation of Micellar Nanoparticles.* Typical procedures employed for the preparation of micellar solution of P(MMA-*co*-NBDAE)$_{56}$-*b*-PF$_9$-*b*-P(MMA-*co*-NBDAE)$_{56}$ triblock copolymer are as follows. 20 mg of ABA triblock copolymer was dissolved in 0.2 mL of THF at first. Into this solution, 99.8 mL of acetone was added via a syringe pump at a flow rate of 1.0 mL/min under vigorous stirring. After the addition is complete, the micellar dispersion was left stirring for another 4 h prior to further fluorescence and UV absorption measurements.

**Characterization.** All $^1$H nuclear magnetic resonance (NMR) spectra were recorded on a Bruker AV300 NMR spectrometer (resonance frequency of 300 MHz for $^1$H) operated in the Fourier transform mode. $CDCl_3$ was used as the solvent. Molecular weights and molecular weight distributions were determined by gel permeation chromatography (GPC) equipped with a Waters 1515 pump and a Waters 2414 differential refractive index detector (set at 30 °C), employing a series of two linear Styragel columns (HR2 and HR4) at an oven temperature of 45 °C. The eluent was THF at a flow rate of 1.0 mL/min. A series of low-polydispersity polystyrene standards were employed for calibration. Dynamic laser light scattering (LLS) measurements were conducted on a commercial spectrometer (ALV/DLS/SLS-5022F) equipped with a multitau digital time correlator (ALV5000) and a cylindrical 22 mW UNIPHASE He−Ne laser ($\lambda_0$ = 632 nm) as the light source. Scattered light was collected at a fixed scattering angle of 90° for duration of ∼5 min. Distribution averages and particle size distributions were computed using cumulants analysis and CONTIN routines. Fluorescence spectra were recorded on F-4600 (Hitachi) spectrofluorometer. The slit widths were both set at 5 nm for excitation and emission, and the excitation wavelength was fixed at 390 nm. All UV−vis spectra were acquired on a RF-5301/PC (Shimadzu) spectrofluorometer.

## RESULTS AND DISCUSSION

**Synthesis of P(MMA-*co*-NBDAE)-*b*-PF-*b*-P(MMA-*co*-NBDAE) Triblock Copolymer.** As shown in Scheme 2, the coil−rod−coil triblock copolymer, P(MMA-*co*-NBDAE)-*b*- PF-*b*-P(MMA-*co*-NBDAE), was synthesized via the ATRP of MMA and NBDAE comonomers by utilizing *Br*-PF$_9$-*Br* as the difunctional initiator. *Br*-PF$_9$-*Br* was synthesized via esterification reaction of *OH*-PF$_9$-*OH* with 2-bromoisobutyryl bromide (Scheme 2). Previously, Huang et al.[63,64] synthesized well-defined coil−rod−coil triblock copolymers by the ATRP of 2-tetrahydropyranyl methacrylate or and 2-(9-carbazolyl)ethyl methacrylate monomer using PF-based ATRP initiator. In the current work, dihydroxyl-terminated PF precursor with a definite DP (9) was employed as the precursor. The chemical structure of *Br*-PF$_9$-*Br* was confirmed by $^1$H NMR in $CDCl_3$ (Figure S1). We can clearly observe that the resonance signal at 4.8 ppm characteristic of terminal hydroxyl protons of *OH*-PF$_9$-*OH* (peak *a*) completely shifted to 5.3 ppm in the NMR spectrum of *Br*-PF$_9$-*Br*. In addition, the appearance of a new resonance signal (peak *b*) at 1.97 ppm is clearly evident. The corresponding integral ratio of peak *a* to PF backbone aryl proton signals at ∼7−8 ppm was determined to be ∼2:27, suggesting the complete end-group transformation of *HO*-PF$_9$-*OH* into *Br*-PF$_9$-*Br* (Figure S1).

The ATRP of MMA and NBDAE comonomers was then conducted in the presence of *Br*-PF$_9$-*Br* difunctional initiator. THF GPC trace of P(MMA-*co*-NBDAE)-*b*-PF$_9$-*b*-P(MMA-*co*-NBDAE) triblock copolymer is shown in Figure S2, revealing a relatively sharp and symmetric peak, giving a number-average molecular weight, $M_{n,GPC}$, of 15.3 kDa and a polydispersity, $M_w/M_n$, of 1.13 (Figure S2). No obvious tailing at the lower molecular weight side can be discerned, indicating the absence of any residues of PF-based macroinitiator. The $^1$H NMR spectrum of the resulting ABA triblock copolymer is shown in Figure S3. The DP of P(MMA-*co*-NBDAE) block was determined to be 56 from the integral ratio of peak *a* to peak *c*, which are characteristic of PF-based macroinitiator and P(MMA-*co*-NBDAE) block, respectively. Thus, the obtained coil−rod−coil ABA triblock copolymer was denoted as P(MMA-*co*-NBDAE)$_{56}$-*b*-PF$_9$-*b*-P(MMA-*co*-NBDAE)$_{56}$.

**FRET Modulation via Micellization of P(MMA-*co*-NBDAE)-*b*-PF-*b*-P(MMA-*co*-NBDAE) Triblock Copolymer in Selective Solvent.** The above synthesized coil−rod−coil ABA triblock copolymer consists of blue-emitting PF middle block and two green-emitting outer P(MMA-*co*-NBDAE) coil blocks. The conjugated PF and NBDAE moieties exhibiting $F^-$ ion-switchable emission characteristics were employed as the FRET donor and acceptor, respectively. Figure S4 shows the emission spectrum of *Br*-PF$_9$-*Br* and the UV absorption spectrum of NBDAE. The former exhibits strong blue emission in the range of 400−500 nm, which overlaps well with the absorption spectrum of NBDAE with a maximum at ∼450 nm. This suggests that this pair of dyes constitute of an excellent FRET pair.

In a common solvent such as THF, both blocks are well-soluble and the ABA triblock copolymer dissolves as unimer chains. The solution exhibits intense blue fluorescence emission. This implies the less contribution of green-emitting NBDAE moieties and suggests that the FRET process is not that effective as expected. This can be interpreted in terms of chemical composition of the triblock copolymer. Actually, one triblock copolymer chain contains one PF block and ∼0.56 NBDAE moiety. Thus, on average, about half of the polymer chains contain no NBDAE dyes. For unimolecularly dissolved triblock chains, the FRET process can only occur for those chains bearing NBDAE, which proceed via the intrachain manner. The FRET process between interchain dyes is less probable to occur due to that they are far apart from each other. We then imagine that triblock copolymer micelles were prepared from the triblock copolymer; the core−shell conformation will render the close proximity between blue-emitting conjugated cores and NBDAE moieties within micellar coronas, leading to the effective occurrence of FRET processes. To fabricate micellar aggregates possessing PF cores and P(MMA-*co*-NBDAE) coronas, selective solvents need to be used. DMF, DMSO, $CH_2Cl_2$, $CHCl_3$, and THF are common solvents for both PF and P(MMA-*co*-NBDAE) blocks. In alcoholic solvents, both blocks are insoluble. Acetone and acetonitrile turn out to be the best choice of selective solvents. In preliminary experiments, comparable sensing performances were obtained for both selective solvents (acetone and acetonitrile). Thus, in subsequent sections, acetone was employed as the selective solvent for the fabrication of triblock copolymer micelles.

To verify this, we checked the evolution of fluorescence emission spectrum of P(MMA-*co*-NBDAE)$_{56}$-*b*-PF$_9$-*b*-P(MMA-*co*-NBDAE)$_{56}$ in THF upon gradual addition of acetone, which is a nonsolvent for the conjugated PF block. From Figure 1, we can observe that in the range of 0−80 vol % acetone the emission

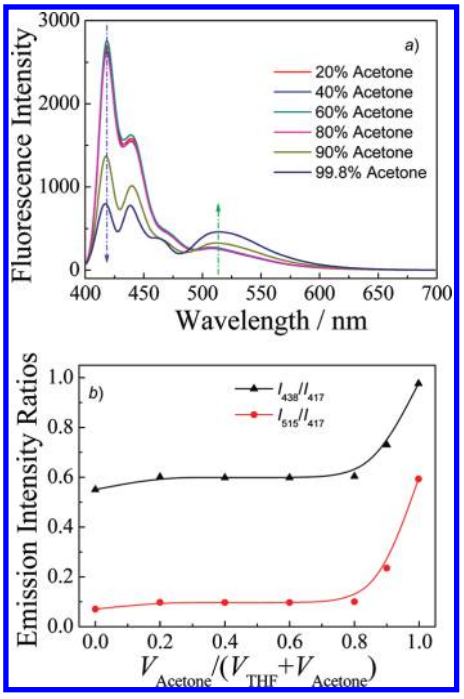


**Figure 1.** (a) Fluorescence emission spectra and (b) fluorescence intensity ratio changes (Ex. 5 nm; Em. 5 nm, $\lambda_{ex}$ = 390 nm) recorded for P(MMA-*co*-NBDAE)$_{56}$-*b*-PF$_9$-*b*-P(MMA-*co*-NBDAE)$_{56}$ triblock copolymer in THF/acetone mixture (0.1 g/L; [PF] = 6.58 $\mu$M, [NBDAE] = 3.68 $\mu$M) with increasing volume fractions of acetone.

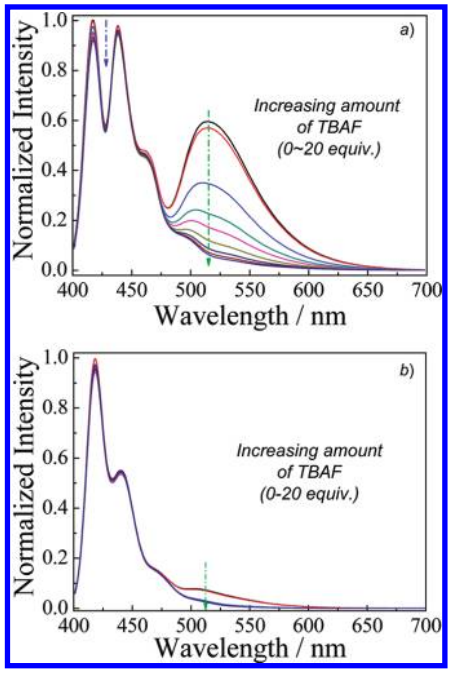


**Figure 2.** Fluorescence spectra recorded for P(MMA-*co*-NBDAE)$_{56}$-*b*-PF$_9$-*b*-P(MMA-*co*- NBDAE)$_{56}$ triblock copolymer (a) micelles in acetone and (b) unimers in THF (0.1 g/L, [PF] = 6.58 $\mu$M, [NBDAE] = 3.68 $\mu$M), respectively, upon addition of 0−20 equiv of TBAF (Ex. 5 nm, Em; 5 nm, $\lambda_{ex}$ = 390 nm).

bands centered at ~417 and 515 nm, which are characteristic of PF and P(MMA-*co*-NBDAE) blocks, respectively, remain essentially unchanged, suggesting that the coil−rod−coil triblock chains still exist in the unimer state. At >80 vol % acetone content, prominent increase in the NBDAE emission and decrease in PF emission can be clearly observed, suggesting the formation of micellar nanoparticles and the occurrence of effective FRET processes. Upon increasing the acetone volume fraction from 20 to 99.8 vol %, the emission intensity ratio, $I_{515}/I_{417}$, increases from 0.070 to 0.593; i.e., ~8.47-fold increase was achieved. A closer examination of Figure 1 further revealed that the decrease of PF blue emission band can be ascribed to two factors, i.e., self-quenching induced by the aggregation of PF block within micellar cores[65,66] and energy transfer to NBDAE moieties within micellar coronas. The former can be monitored by the changes in the emission intensity ratios of $I_{438}/I_{417}$, which agrees well with previous literature reports.[65,66] In addition, the prominent increase of NBDAE green emission at >80 vol % acetone can be safely ascribed to the FRET mechanism between core-forming PF block and NBDAE moieties in micellar coronas. The above analysis further confirmed that the FRET principle can be facilely employed for the sensitive monitoring of block copolymer micellization process. The formation of micelles consisting of PF cores and P(MMA-*co*-NBDAE) coronas was further confirmed by dynamic LLS measurements, and the results are shown in Figure S5. Dynamic LLS revealed an intensity-average hydrodynamic radius, $\langle R_h \rangle$, of 28.4 nm and a size polydispersity, $\mu_2/\Gamma^2$, of 0.119.

**P(MMA-*co*-NBDAE)-*b*-PF-*b*-P(MMA-*co*-NBDAE) Triblock Copolymer Micelles and Unimer Chains as Ratiometric Fluorometric Probes of Fluoride Ions.** In this section, we further investigated the ratiometric fluorescent $F^-$-sensing capability of P(MMA-*co*-NBDAE)$_{56}$-*b*-PF$_9$-*b*-P(MMA-*co*-NBDAE)$_{56}$ triblock copolymer in the unimer and micellar states, respectively. We have previously established that NBDAE and NBDAE-containing polymers can serve fluorometric $F^-$ probes with the detection limit down to ~0.8 $\mu$M.[40] Two different mechanisms, HB interactions and deprotonation via Brønsted acid−base interaction, are responsible for the fluorescence quenching at low and high $F^-$ concentrations, respectively.

Upon addition of varying amount of TBAF (0−20 equiv relative to NBDAE moieties) into the THF solution of P(MMA-*co*-NBDAE)$_{56}$-*b*-PF$_9$-*b*-P(MMA-*co*-NBDAE)$_{56}$ triblock unimers, we can apparently observe that the characteristic NBDAE emission band centered at ~515 nm, though quite weak, almost completely disappeared (Figure 2b). This agrees quite well with the previous work concerning $F^-$ ion-induced fluorescent quenching of NBDAE and NBDAE-containing polymers.[40] On the other hand, the emission of PF block remains almost unaltered. The latter was further confirmed by control experiments which revealed that the PF emission is almost independent of externally added TBAF in the same concentration range (Figure S6). It is worth noting that for coil−rod−coil triblock unimers in THF in the absence of TBAF the quite weak NBDAE emission band should be ascribed to the fact that NBDAE moieties exhibit quite weak absorbance at the excitation wavelength (390 nm) (Figure S4). From Figure 3, we can tell that in the range of 0−4.0 equiv of TBAF the emission intensity ratio, $I_{515}/I_{417}$, decreases from 0.070 to 0.024; i.e., ~2.92-fold decrease in the emission intensity ratio was achieved. At >4.0 equiv of TBAF, the $I_{515}/I_{417}$ ratio does not exhibit any further changes. Also note that for triblock unimers in the absence or presence TBAF the PF blue emission dominates in both cases; thus, visual inspection of the presence of $F^-$ ions is not possible due to the lack of any appreciable fluorometric transition.

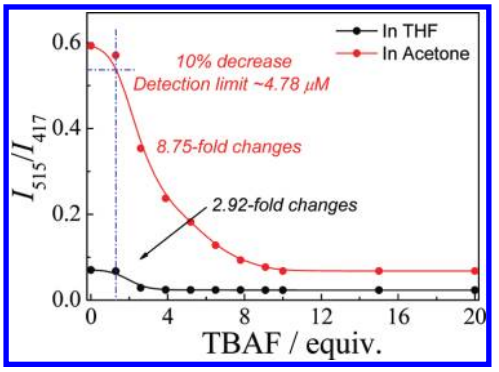


**Figure 3.** Fluorescence emission intensity ratio changes recorded for P(MMA-*co*- NBDAE)$_{56}$-*b*-PF$_9$-*b*-P(MMA-*co*-NBDAE)$_{56}$ micelles in acetone and unimers in THF (0.1 g/L, [PF] = 6.58 $\mu$M, [NBDAE] = 3.68 $\mu$M), respectively, upon addition of 0−20 equiv of TBAF (Ex. 5 nm; Em. 5 nm, $\lambda_{ex}$ = 390 nm).

For P(MMA-*co*-NBDAE)$_{56}$-*b*-PF$_9$-*b*-P(MMA-*co*-NBDAE)$_{56}$ triblock copolymer micelles in acetone (containing 0.2 vol % THF), effective FRET process occurs between the core-forming PF core and NBDAE moieties in the corona, leading to the relatively high $I_{515}/I_{417}$ emission intensity ratio of 0.593 (Figure 2a). Upon addition of varying amount of TBAF in the range of 0−20 equiv relative to NBDAE moieties, the diagnostic emission band of NBDAE moieties at ∼515 nm is gradually quenched; this is also accompanied by colorimetric change from green to yellowish under visible light and fluorometric transition from cyan to blue under UV 365 nm irradiation, respectively (Scheme 1 and Figure 2a). As opposed to that in pure THF, in which 4.0 equiv of TBAF can lead to the almost complete quenching of NBDAE emission band (Figure 2b), ∼10.0 equiv of TBAF is needed to fully quench the NBDAE emission for triblock copolymer micellar solution (Figures 2a and 3). In the range of 0−10 equiv of TBAF, fluorescence emission intensity ratio ($I_{515}/I_{417}$) changed from 0.593 to 0.0678 (Figure 3). Thus, the emission intensity ratio exhibits ∼8.75-fold changes upon TBAF addition.

To further confirm the existence of FRET process between PF cores and NBDAE-containing coronas within triblock micelles and its contribution to the sensitivity enhancement, fluorescence emission spectra were collected at varying excitation wavelengths. Upon excitation at 390 nm, we can apparently observe well-resolved emission peaks of blue-emitting PF cores and green-emitting NBDAE moieties in the micellar coronas. Upon excitation at 450 nm, which can not effectively excite PF cores compared to that by 390 nm excitation, only the green emission of NBDAE moieties can be discerned. Most importantly, compared to that excited at 450 nm, ∼2.78-fold enhancement in the NBDAE emission band at ∼515 nm was observed when excited at 390 nm (Figure S7a). Considering that in the absence of fluoride ions NBDAE moieties possess considerably higher absorbance at 450 nm compared to that at 390 nm (Figure S8) and the fact that NBDAE is a weak green-emitter when excited at 390 nm (Figure S4), we can safely conclude that effective FRET processes occur between PF cores and NBDAE-containing coronas when excited at 390 nm. Figure S7b revealed that in the presence of 0−20 equiv of TBAF the NBDAE emission bands exhibit ∼40-fold and 9.5-fold decrease when excited at 390 and 450 nm, respectively. This suggests that fluoride ion-induced intensity changes in the NBDAE emission band only can be well employed for the sensitive fluorometric $F^-$ sensing. We can also

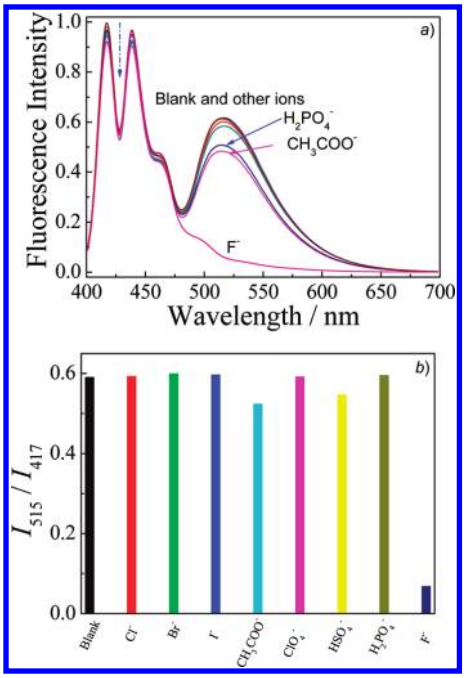


**Figure 4.** (a) Fluorescence spectra and (b) fluorescence intensity ratio changes of micellar solution of P(MMA-*co*-NBDAE)$_{56}$-*b*-PF$_9$-*b*-P(MMA-*co*-NBDAE)$_{56}$ triblock copolymer in acetone (0.1 g/L, 2 mL, [PF] = 6.58 $\mu$M, [NBDAE] = 3.68 $\mu$M) in the presence of 10 equiv (20 $\mu$L acetone solution) of tetra-*n*-butylammonium (TBA) salts of $Cl^-$, $Br^-$, $I^-$, $CH_3COO^-$, $ClO_4^-$, $HSO_4^-$, $H_2PO_4^-$, and $F^-$ (Ex. 5 nm; Em. 5 nm, $\lambda_{ex}$ = 390 nm).

infer from the above results that the integration of FRET processes between micellar cores and coronas into the polymeric sensor, when excited at 390 nm, can considerably boost the detection sensitivity.

From the results shown in Figure 3, we can conclude that P(MMA-*co*- NBDAE)$_{56}$-*b*-PF$_9$-*b*-P(MMA-*co*-NBDAE)$_{56}$ triblock copolymer micelles in acetone exhibit much better ratiometric fluorescent $F^-$ ion-sensing performance as they exhibit ∼8.75-fold changes in emission intensity ratios upon TBAF addition, which is much higher that exhibited by triblock unimer chains in THF (∼2.92-fold decrease in emission intensity ratios). The former also renders possible the visual detection of $F^-$ ions due to that for unimolecularly dissolved triblock chains in THF the blue emission of PF block always dominates in the presence and absence of $F^-$ ions. Again, this further strengthened the advantage of employing coil−rod−coil triblock copolymer micelles as the ratiometric fluorescent $F^-$ sensing platform. If we arbitrarily define the detection limit as the $F^-$ concentration at which a 10% decrease in fluorescence emission intensity ratio can be measured by employing 0.1 g/L micellar solution of P(MMA-*co*-NBDAE)$_{56}$-*b*-PF$_9$-*b*-P(MMA-*co*-NBDAE)$_{56}$, the detection limit of $F^-$ ions was determined to be ∼4.78 $\mu$M (Figure 3), which is much lower than the EPA standard set for drinking water (210 $\mu$M).[67]

From Figure S8, we can tell that upon gradual addition of TBAF in the range of 0−20 equiv the maximum NBDAE absorption band centered at ∼450 nm red shifts to ∼455 nm accompanied by the appearance and increase in intensity of two new absorption peaks at 395 and 409 nm. A closer examination of Figure 2a,b revealed that upon TBAF addition the characteristic PF emission band for both triblock unimer and micellar solutions exhibits a slight decrease. We ascribe this to changes in the

absorbance of NBDAE moieties induced by TBAF. As shown in Figures S4 and S8, the interaction of TBAF with NBDAE moieties leads to the appearance of a new absorption peak centered at around 400 nm. Thus, there exists partial energy transfer between PF emission and the newly emerged NBDAE absorption.

To assess the $F^-$ ion sensing selectivity of P(MMA-*co*-NBDAE)$_{56}$-*b*-PF$_9$-*b*-P(MMA- *co*-NBDAE)$_{56}$ micelles over other common anions, further competition experiments were conducted (Figure 4). Acetone solution (10 equiv, 20 $\mu$L) of tetrabutylammonium (TBA) salts of $Cl^-$, $Br^-$, $I^-$, $CH_3COO^-$, $ClO_4^-$, $HSO_4^-$, $H_2PO_4^-$, and $F^-$ were respectively added into 2.0 mL of micellar solution of P(MMA-*co*-NBDAE)$_{56}$-*b*-PF$_9$-*b*-P(MMA-*co*-NBDAE)$_{56}$ in acetone. Among them, only the addition of TBAF resulted in prominent quenching of NBDAE emission band, accompanied by fluorescence intensity ratio ($I_{515}/I_{417}$) changes from 0.593 to 0.070 (Figure 4). Most importantly, though $H_2PO_4^-$ and $CH_3COO^-$ ions often act as competitive ions during the sensing of $F^-$ ions, in the current system, the presence of 10.0 equiv of $H_2PO_4^-$ and $CH_3COO^-$ did not incur significant changes in emission intensity ratios, as compared to that induced by TBAF.

In the current case, both PF and P(MMA-*co*-NBDAE) blocks of the triblock copolymer are hydrophobic. This poses considerable limitations considering that practical applications of fluorometric $F^-$ ion sensing systems are often associated with aqueous samples or need to be conducted in aqueous milieu. Moreover, the recognition and interaction of $F^-$ ions with NBDAE moieties are quite reversible in nature and highly dependent on the presence of water. Previous report indicated that the presence of ~10% (v/v) water can almost completely recover the NBDAE fluorescence emission initially quenched by $F^-$ ions.[40] Future works toward this aspect, including the fabrication of fluorometric and colorimetric $F^-$ probes compatible with pure aqueous media by integrating with water-soluble polymers, are currently underway.

## CONCLUSIONS

Well-defined coil−rod−coil ABA triblock copolymer, P(MMA-*co*-NBDAE)$_{56}$-*b*-PF$_9$-*b*-P(MMA-*co*-NBDAE)$_{56}$, was synthesized via the ATRP technique. Within the triblock copolymer, blue-emitting conjugated PF block and $F^-$-sensitive green-emitting NBDAE moieties within the PMMA block can serve as FRET donors and switchable acceptors, respectively. In a good solvent such as THF, the blue emission of PF block dominates due to the unimolecularly dissolved state. The addition of $F^-$ ions only leads to ~2.92-fold decrease ($I_{515}/I_{417}$) in fluorescence intensity ratios, and no apparent emission color changes can be discerned by the naked eye when checked under UV 365 nm irradiation. In acetone, the triblock copolymer spontaneously self-assembles into micelles possessing PF cores and NBDAE-labeled PMMA coronas. In the absence of $F^-$ ions, effective FRET processes between micellar cores and coronas occurs, resulting in prominently enhanced NBDAE emission. Upon addition of $F^-$ ions, the quenching of NBDAE emission bands leads to ~8.75-fold decrease of the emission intensity ratio ($I_{515}/I_{417}$), and this process can be visually checked by the naked eye from the fluorometric transition from cyan to blue emission and colorimetric transition from green to yellowish. This work demonstrated that micelles constructed from coil−rod−coil triblock copolymers can serve as ratiometric fluorescent $F^-$ ion sensors with better performance than molecularly dissolved unimer chains upon proper structural design and optimization of the spatial distribution of FRET donors and acceptors.

## ASSOCIATED CONTENT

**Supporting Information.** $^1$H NMR, GPC, UV−vis absorption spectra, and fluorescence spectra. This material is available free of charge via the Internet at http://pubs.acs.org.

## AUTHOR INFORMATION

**Corresponding Author**
*E-mail: sliu@ustc.edu.cn (S.L.), yhgeng@ciac.jl.cn (Y.G.).

## ACKNOWLEDGMENT

The financial support from National Natural Scientific Foundation of China (NNSFC) Project (20874092, 91027026, and 51033005) and Fundamental Research Funds for the Central Universities is gratefully acknowledged.

## REFERENCES

(1) Kubik, S. *Chem. Soc. Rev.* **2009**, *38*, 585–605.
(2) Li, A. F.; Wang, J. H.; Wang, F.; Jiang, Y. B. *Chem. Soc. Rev.* **2010**, *39*, 3729–3745.
(3) Gale, P. A.; Garcia-Garrido, S. E.; Garric, J. *Chem. Soc. Rev.* **2008**, *37*, 151–190.
(4) Schmidtchen, F. P.; Berger, M. *Chem. Rev.* **1997**, *97*, 1609–1646.
(5) O'Neil, E. J.; Smith, B. D. *Coord. Chem. Rev.* **2006**, *250*, 3068–3080.
(6) Gunnlaugsson, T.; Glynn, M.; Tocci, G. M.; Kruger, P. E.; Pfeffer, F. M. *Coord. Chem. Rev.* **2006**, *250*, 3094–3117.
(7) Gale, P. A.; Quesada, R. *Coord. Chem. Rev.* **2006**, *250*, 3219–3244.
(8) Beer, P. D.; Gale, P. A. *Angew. Chem., Int. Ed.* **2001**, *40*, 486–516.
(9) Takeuchi, M.; Shioya, T.; Swager, T. M. *Angew. Chem., Int. Ed.* **2001**, *40*, 3372–3376.
(10) Kim, E.; Kim, H. J.; Bae, D. R.; Lee, S. J.; Cho, E. J.; Seo, M. R.; Kim, J. S.; Jung, J. H. *New J. Chem.* **2008**, *32*, 1003–1007.
(11) Zhao, Y. P.; Zhao, C. C.; Wu, L. Z.; Zhang, L. P.; Tung, C. H.; Pan, Y. J. *J. Org. Chem.* **2006**, *71*, 2143–2146.
(12) Kim, T. H.; Choi, M. S.; Sohn, B. H.; Park, S. Y.; Lyoo, W. S.; Lee, T. S. *Chem. Commun.* **2008**, 2364–2366.
(13) Cho, E. J.; Moon, J. W.; Ko, S. W.; Lee, J. Y.; Kim, S. K.; Yoon, J.; Nam, K. C. *J. Am. Chem. Soc.* **2003**, *125*, 12376–12377.
(14) Kim, S. K.; Bok, J. H.; Bartsch, R. A.; Lee, J. Y.; Kim, J. S. *Org. Lett.* **2005**, *7*, 4839–4842.
(15) Cho, E. J.; Ryu, B. J.; Lee, Y. J.; Nam, K. C. *Org. Lett.* **2005**, *7*, 2607–2609.
(16) Sessler, J. L.; Black, C. B.; Andrioletti, B.; Try, A. C.; Ruiperez, C. *J. Am. Chem. Soc.* **1999**, *121*, 10438–10439.
(17) Anzenbacher, P.; Jursikova, K.; Sessler, J. L. *J. Am. Chem. Soc.* **2000**, *122*, 9350–9351.
(18) Sessler, J. L.; Mizuno, T.; Wei, W. H.; Eller, L. R. *J. Am. Chem. Soc.* **2002**, *124*, 1134–1135.
(19) He, X. M.; Hu, S. Z.; Liu, K.; Guo, Y.; Xu, J.; Shao, S. J. *Org. Lett.* **2006**, *8*, 333–336.
(20) Maeda, H.; Haketa, Y.; Nakanishi, T. *J. Am. Chem. Soc.* **2007**, *129*, 13661–13674.
(21) Xie, Y. S.; Wang, Q. G.; Ding, Y. B.; Li, X.; Zhu, W. H. *Chem. Commun.* **2010**, *46*, 3669–3671.
(22) Qu, Y.; Hua, J. L.; Tian, H. *Org. Lett.* **2010**, *12*, 3320–3323.
(23) Jiang, J. B.; Xiao, X.; Zhao, P.; Tian, H. *J. Polym. Sci., Part A: Polym. Chem.* **2010**, *48*, 1551–1556.
(24) Hudson, Z. M.; Wang, S. N. *Acc. Chem. Res.* **2009**, *42*, 1584–1596.
(25) Melaimi, M.; Gabbai, F. P. *J. Am. Chem. Soc.* **2005**, *127*, 9680–9681.

(26) Liu, X. Y.; Bai, D. R.; Wang, S. N. *Angew. Chem., Int. Ed.* **2006**, *45*, 5475–5478.
(27) Yamaguchi, S.; Shirasaka, T.; Akiyama, S.; Tamao, K. *J. Am. Chem. Soc.* **2002**, *124*, 8816–8817.
(28) Yamaguchi, S.; Akiyama, S.; Tamao, K. *J. Am. Chem. Soc.* **2000**, *122*, 6793–6794.
(29) Saxena, A.; Fujiki, M.; Rai, R.; Kim, S. Y.; Kwak, G. *Macromol. Rapid Commun.* **2004**, *25*, 1771–1775.
(30) Arimori, S.; Davidson, M. G.; Fyles, T. M.; Hibbert, T. G.; James, T. D.; Kociok-Kohn, G. I. *Chem. Commun.* **2004**, 1640–1641.
(31) Xu, S.; Chen, K. C.; Tian, H. *J. Mater. Chem.* **2005**, *15*, 2676–2680.
(32) Yang, X. F.; Ye, S. J.; Bai, Q.; Wang, X. Q. *J. Fluoresc.* **2007**, *17*, 81–87.
(33) Hu, R.; Feng, J. A.; Hu, D. H.; Wang, S. Q.; Li, S. Y.; Li, Y.; Yang, G. Q. *Angew. Chem., Int. Ed.* **2010**, *49*, 4915–4918.
(34) Kim, T. H.; Swager, T. M. *Angew. Chem., Int. Ed.* **2003**, *42*, 4803–4806.
(35) Kim, S. Y.; Hong, J. I. *Org. Lett.* **2007**, *9*, 3109–3112.
(36) Lee, C. H.; Sokkalingam, P. *J. Org. Chem.* **2011**, *76*, 3820–3828.
(37) Bai, R. K.; Bao, Y. Y.; Liu, B.; Wang, H.; Tian, J. A. *Chem. Commun.* **2011**, *47*, 3957–3959.
(38) Park, S. B.; Kim, S. Y.; Park, J.; Koh, M.; Hong, J. I. *Chem. Commun.* **2009**, 4735–4737.
(39) Akkaya, E. U.; Bozdemir, O. A.; Sozmen, F.; Buyukcakir, O.; Guliyev, R.; Cakmak, Y. *Org. Lett.* **2010**, *12*, 1400–1403.
(40) Hu, J. M.; Li, C. H.; Cui, Y.; Liu, S. Y. *Macromol. Rapid Commun.* **2011**, *32*, 610–615.
(41) Hu, J. M.; Liu, S. Y. *Macromolecules* **2010**, *43*, 8315–8330.
(42) Yoon, J.; Kim, H. N.; Guo, Z. Q.; Zhu, W. H.; Tian, H. *Chem. Soc. Rev.* **2011**, *40*, 79–93.
(43) Zhao, P.; Jiang, J. B.; Leng, B.; Tian, H. *Macromol. Rapid Commun.* **2009**, *30*, 1715–1718.
(44) McQuade, D. T.; Pullen, A. E.; Swager, T. M. *Chem. Rev.* **2000**, *100*, 2537–2574.
(45) Swager, T. M.; Thomas, S. W.; Joly, G. D. *Chem. Rev.* **2007**, *107*, 1339–1386.
(46) Swager, T. M. *Acc. Chem. Res.* **1998**, *31*, 201–207.
(47) Yin, J.; Hu, H. B.; Wu, Y. H.; Liu, S. Y. *Polym. Chem.* **2011**, *2*, 363–371.
(48) Hu, J. M.; Dai, L.; Liu, S. Y. *Macromolecules* **2011**, *44*, 4699–4710.
(49) Wan, X. J.; Zhang, G. Y.; Liu, S. Y. *Macromol. Rapid Commun.* **2011**, *32*, 1082–1089.
(50) Wang, D.; Liu, T.; Yin, J.; Liu, S. Y. *Macromolecules* **2011**, *44*, 2282–2290.
(51) Liu, T.; Liu, S. Y. *Anal. Chem.* **2011**, *83*, 2775–2785.
(52) Wan, X. J.; Liu, T.; Liu, S. Y. *Langmuir* **2011**, *27*, 4082–4090.
(53) Li, C. H.; Hu, J. M.; Liu, T.; Liu, S. Y. *Macromolecules* **2011**, *44*, 429–431.
(54) Wan, X. J.; Wang, D.; Liu, S. Y. *Langmuir* **2010**, *26*, 15574–15579.
(55) Li, C. H.; Liu, S. Y. *J. Mater. Chem.* **2010**, *20*, 10716–10723.
(56) Hu, J. M.; Li, C. H.; Liu, S. Y. *Langmuir* **2010**, *26*, 724–729.
(57) Liu, T.; Hu, J. M.; Yin, J.; Zhang, Y. F.; Li, C. H.; Liu, S. Y. *Chem. Mater.* **2009**, *21*, 3439–3446.
(58) Hu, R.; Feng, J. A.; Hu, D. H.; Wang, S. Q.; Li, Y.; Yang, G. Q. *Angew. Chem., Int. Ed.* **2010**, *49*, 4915–4918.
(59) Huang, L.; Wu, S. P.; Qu, Y.; Geng, Y. H.; Wang, F. S. *Macromolecules* **2008**, *41*, 8944–8947.
(60) Liu, Q.; Qu, Y.; Geng, Y. H.; Wang, F. S. *Macromolecules* **2008**, *41*, 5964–5966.
(61) Wu, T.; Zou, G.; Hu, J. M.; Liu, S. Y. *Chem. Mater.* **2009**, *21*, 3788–3798.
(62) Li, C. H.; Zhang, Y. X.; Hu, J. M.; Cheng, J. J.; Liu, S. Y. *Angew. Chem., Int. Ed.* **2010**, *49*, 5120–5124.
(63) Lu, S.; Fan, Q. L.; Liu, S. Y.; Chua, S. J.; Huang, W. *Macromolecules* **2002**, *35*, 9875–9881.
(64) Lu, S.; Fan, Q. L.; Chua, S. J.; Huang, W. *Macromolecules* **2003**, *36*, 304–310.
(65) Leclerc, M. *J. Polym. Sci., Part A: Polym. Chem.* **2001**, *39*, 2867–2873.
(66) Scherf, U.; List, E. J. W. *Adv. Mater.* **2002**, *14*, 477–487.
(67) Gabbai, F. P.; Kim, Y. *J. Am. Chem. Soc.* **2009**, *131*, 3363–3369.